Int. J. Heat Mass Transfer. Vol. 36, No. 1, pp. 227–231, 1993
Printed in Great Britain

0017–9310/93 $5.00 + 0.00

TECHNICAL NOTES

Critical heat flux hysteresis in vapor–liquid counterflow in porous media

A. K. STUBOS, C. SATIK and Y. C. YORTSOS†
Department of Chemical Engineering, Petroleum Engineering Program, University of Southern California, Los Angeles, CA 90089-1211, U.S.A.

(*Received* 3 *July* 1991 *and in final form* 25 *November* 1991)

INTRODUCTION

IN A RECENT study on steady-state counterflow in porous media, Satik *et al.* [1] presented a unified description of the process including capillarity, conduction and Kelvin effects. The separate contexts in which these phenomena have been analyzed before, namely heat pipe [2] and geothermal [3], result as limiting cases of this unified approach. In the present communication, the physical implications of the work by Satik *et al.* are further discussed leading to an improved understanding of boiling and geothermal applications and the relevance of the critical heat flux.

To proceed, it is briefly noted that in the notation of Satik *et al.* [1] temperature and saturation profiles are obtained from the following system:

$$\frac{d\tau}{d\xi} = \frac{H(\tau, S)}{F(\tau, S)} \tag{1}$$

$$\frac{dS}{d\xi}\frac{dJ}{dS} = \frac{G(\tau, S)}{F(\tau, S)} \tag{2}$$

where H and F are positive functions. The important function is G which can change sign somewhere in the (τ, S) space:

$$G = k_{rl}(\sin\theta R_l + \omega K R_m A/\tau^2 + \sin\theta k_{rv} K R_m A/\tau^2) + \beta k_{rv}(\sin\theta R_v + \omega K R_m A/\tau^2). \tag{3}$$

Here, vapor pressure lowering has been excluded without loss. The various dimensionless variables and parameters were defined in ref. [1]. We simply recall that coordinate ξ increases in the direction from the liquid to the vapor, $\omega = q\mu_v/kL_v g\Delta\rho\rho_v$ is a dimensionless heat flux, and $KR_m = kL_v^2 M_w P_{in}\rho_v/\mu_v \lambda R T_0^2$ measures the effect of heat conduction. The angle θ is measured counterclockwise, such that vapor is at the bottom or the top when $\theta = 3\pi/2$ or $\pi/2$, respectively.

The above is a set of two ordinary differential equations, the solution of which requires two boundary conditions. In principle, a two-point boundary value problem can be specified. However, this necessitates that the length of integration be known a priori. This is rarely the case. Instead, the problem is typically viewed as an initial value problem, in which temperature and saturation are specified at one end and integration proceeds towards the opposite end.

STEADY-STATE VERTICAL COUNTERFLOW

The case where heat flows from the bottom to the top involves two applications. In boiling, a subcooled liquid region exists at the top, while it is not necessary that a dry region exists at the bottom. Saturation temperature and $S = 1$ are imposed at the interface II–III and integration proceeds in the positive ξ direction (Fig. 1(a)). Some geothermal systems, on the other hand, contain superheated vapor at the bottom but not necessarily subcooled liquid at the top. Thus, saturation temperature and $S = 0$ are imposed in region I, the integration now proceeding in the negative ξ direction (Fig. 1(b)). This latter case was thoroughly analyzed in ref. [1].

In either case, a critical heat flux ω_{cr} can be defined. In boiling, it denotes the minimum value for the first appearance of a dry region (I) at the bottom. In the geothermal application, it is the minimum value necessary to sustain a liquid zone (III) at the top. However, although the two configurations are practically the same, the profiles obtained and the critical heat flux value in the two systems are quite different. This difference is the main subject of this note.

Consider, first, the boiling case. Physically, one starts from an initially liquid-saturated medium, through which heat is conducted, and the top surface of which is maintained at constant temperature. Above a certain value of q, boiling is initiated. A liquid-two phase (II–III) interface develops at some distance from the top. Integration for the underlying two-phase region starts here ($S = 1$). Then the following apply: for $\omega > \omega_{cr}$, a finite length boiling region (spanning the entire saturation interval) may develop. However, this length is unbounded when $\omega < \omega_{cr}$.

In theory, dryout would occur when ω first reaches ω_{cr}. It should be pointed out that this only represents a lower limit. In practice (e.g. experiments similar to those reported in refs. [2, 4]), the two-phase zone length is given by the difference between the total and the conductive height. Thus, the thickness available in the experiment to the two-phase zone must be larger than the theoretical prediction for dryout. As a result, the dryout heat flux value will be typically greater than ω_{cr}.

In the limit of negligible conduction in the two-phase zone ($KR_m \gg 1$), ω_{cr} is equal to a constant ω_0 [2], which does not depend on process parameters (e.g. it takes the value 0.3063 for a specific pair of relative permeabilities used for steam–water). When additionally $\omega < \omega_0$, equations (1)–(3) show that two possible solutions exist, each with a nearly flat saturation profile (Fig. 2). The saturation values corresponding to each of these are obtained from solving $G = 0$, which here simply reads

$$\omega = \frac{k_{rl}k_{rv}}{k_{rl} + \beta k_{rv}}. \tag{4}$$

This condition expresses the physical situation of equal vapor and liquid pressure gradients ($dP_c = 0$), i.e. the counterflow is driven by gravity alone. The nearly flat profiles are the attractors of trajectories emanating from either the vapor (vapor-dominated, VD) or the liquid (liquid-dominated, LD) sides, respectively (Fig. 2). Capillarity is important in the spatially short zone that connects dry or subcooled liquid regions with the attracting profile. Which trajectory is selected depends only on the specification of the boundary con-

†Author to whom correspondence should be addressed.

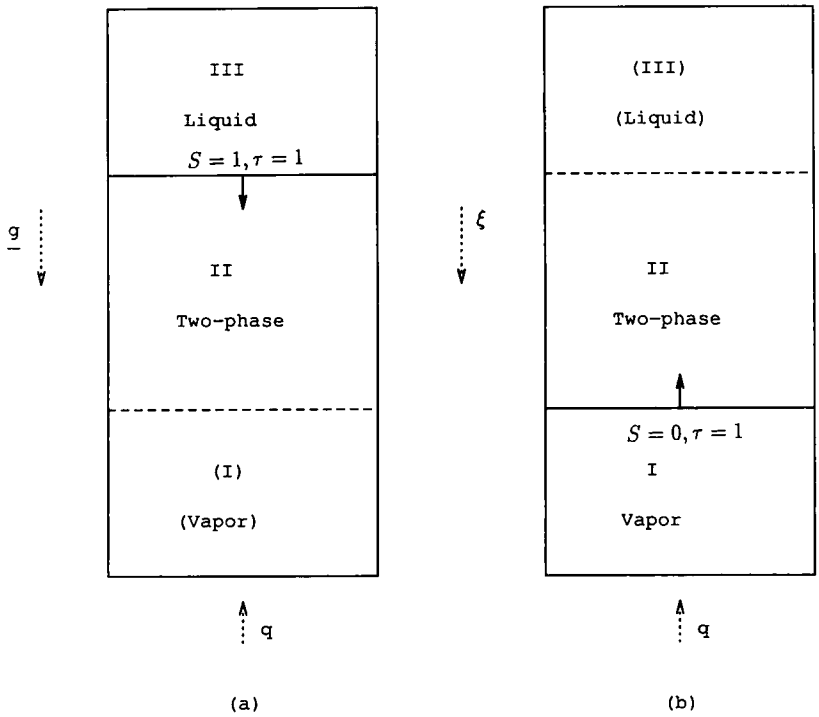

FIG. 1. Schematics of vapor–liquid counterflow for (a) boiling, (b) geothermal systems. Arrows indicate the direction of integration.

dition. In the present boiling application, it is the LD solution (the one with the largest saturation value) that is followed.

We should point out that, while appropriate for the most part, such solutions are physically inconsistent at the bottom boundary. Indeed, since the two-phase zone must end there, its extent is finite. In the present formalism, this can only be accomplished by terminating the nearly flat profile at the appropriate point. However, this results in non-zero fluxes of both liquid and vapor at the impermeable bottom boundary, as can be readily shown. The effect is certainly non-physical and must be removed. The paradox persists even if conduction, capillarity and vapor pressure lowering are included, as indeed considered below. How can we resolve this paradox? One possibility is that a true 1D steady state may not exist for $\omega < \omega_{cr}$. This was alluded to in ref. [1]. Another is that the present 1D formalism is inapplicable near

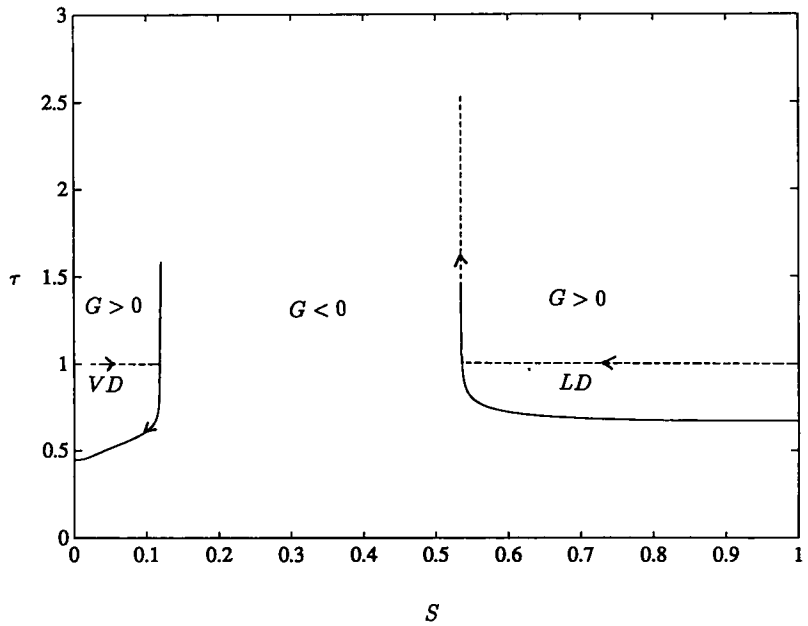

FIG. 2. Solution trajectories (dashed curves) for $\omega = 0.1$. Solid curves correspond to $G = 0$ (to which trajectories are attracted). Arrows indicate the direction of integration.

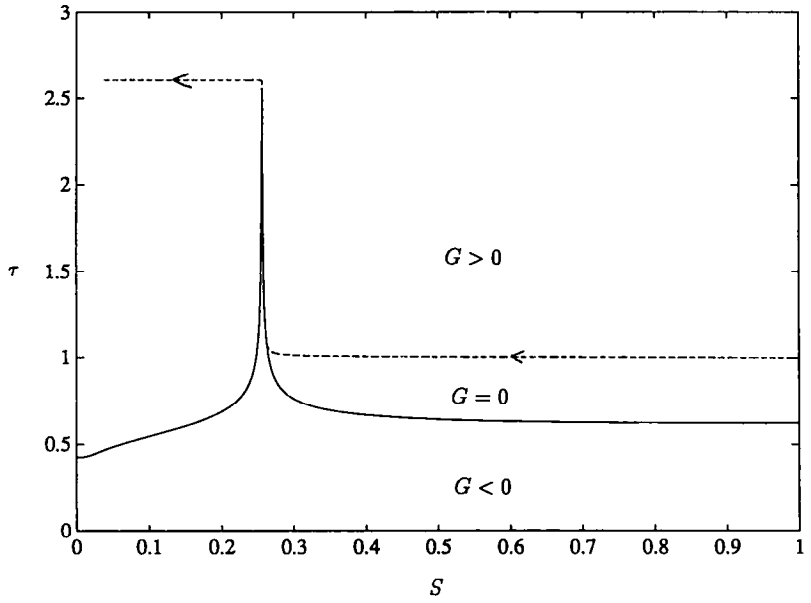

FIG. 3. Solution trajectory (dashed curve) for $\omega = 0.3065$ and $KR_m = 1031$. The solid curve corresponds to $G = 0$. Arrows indicate the direction of integration.

the bottom boundary, and must be modified by using a more detailed 2D analysis, e.g. a pore network model. For a real system, a third possibility is to invoke an appropriate heterogeneity in permeability somewhere in the system. All these are currently under study.

For finite KR_m, ω_{cr} departs from ω_0 due to conduction and the curve $G = 0$ depends also on T

$$\frac{\omega}{1+\dfrac{1}{k_{rv}KR_mA/\tau^2}} \equiv \frac{\omega}{1+\dfrac{q_{cond}}{q_{conv}}} = \frac{k_{rl}k_{rv}}{k_{rl}+\beta k_{rv}}. \tag{5}$$

Nevertheless, as long as $\omega < \omega_0$, the profile still corresponds to the flat saturation (LD) value found above. For a value of ω very slightly above ω_0, the curve $G = 0$ no longer consists of two segments parallel to the τ axis, which have now merged to produce the shape of Fig. 3. For the conditions of Fig. 3 ($\omega = 0.3065$) it is possible for the solution to span the entire saturation range, i.e. for a finite zone to exist, but an almost flat saturation profile can still be theoretically sustained for a significant depth. The physical reason for this behavior is that although temperature increases, and at a growing rate as the $G = 0$ curve is approached, the temperature gradients are still small ($(dT/dP)_c$ is small). Thus, the conductive flux, q_{cond}, is small compared with the convective flux, q_{conv}. In this sense, a monotonic saturation profile can be obtained. Now, the critical threshold has been surpassed ($\omega > \omega_{cr}$) and dryout is possible. For slightly larger values of ω (e.g. for $\omega > 0.308$), however, the sharp peak of the $G = 0$ curve of Fig. 3 diminishes fast, making it possible for the integration to reach the dry limit ($S = 0$) in a considerably shorter distance. The resulting trajectories are very similar to Fig. 6 of ref. [1].

The critical flux for boiling as a function of KR_m was calculated (equivalently, as a function of permeability, Fig. 4). It was found that ω_{cr} differs very little from the asymptote ω_0 of ref. [2], unless the permeability becomes extremely low or the conductivity extremely high ($KR_m \to 0$). In that limit, however, the heat flux is conducted rather than convected. This effect is limited to a rather unusual region, therefore it can be ignored for most practical cases. This behavior of ω_{cr} for boiling is consistent with previous studies, but differs significantly from that of Satik *et al.* [1], who predicted not only a substantial effect of KR_m, but also the existence of a critical value, k_h, near which ω_{cr} diverges.

In order to understand this difference let us remark that the problem investigated by Satik *et al.* [1] may be physically related to a different process, namely condensation. An initially vapor-occupied region is progressively cooled at the top, the bottom being kept at constant temperature. Above a certain value of q, condensation is initiated. If $\omega < \omega_0$, the system behaves similarly to what was described above, except that now it is the VD solution that is reached (see Fig. 2). As in the previous, the solution is incompatible at the top end, where the indefinitely growing two-phase zone must be terminated. Satik *et al.* conjectured against the existence of a steady state under such conditions.

In the no-conduction limit, ω_{cr} coincides with ω_0. However, when KR_m is finite, ω_{cr} is significantly different from ω_0. For a physical explanation, we note that when $\omega_0 < \omega < \omega_{cr}$, the conductive heat flux becomes progressively more important (larger $(dT/dP)_c$) as the solution trajectory proceeds towards higher saturations and lower temperatures (Fig. 5 of Satik *et al.*). When it intersects the curve $G = 0$, the temperature gradient has reached a value such that $q_{cond} = q$. At this point, the saturation profile goes through a maximum and the solution enters the region $G < 0$. From then on, the directions of vapor and liquid velocities in the boiling region are reversed resulting in negative convective heat flux so that heat balance is satisfied. This condition was also deemed unphysical by Satik *et al.* [1], who postulated the existence of steady states only for $\omega > \omega_{cr}$.

In addition to being sensitive to KR_m, the critical heat flux becomes infinitely large as the permeability k approaches a threshold value k_b (Fig. 4). This is due to the vanishing of the vapor pressure. Indeed, as the permeability gets lower, capillarity (and gravity to a lesser extent) impose large pressure drops in the upwards direction, ultimately resulting in negative P_v values. Then, k_b denotes the lowest permeability value below which steady-state counterflow cannot be sustained. This limiting value varies linearly with $(\sigma/P_0)^2$ and is independent of the thermal conductivity λ [1].

The difference between the two ω_{cr} curves suggests an effect of hysteresis. In the boiling case, an initially liquid-filled medium is converted to a vapor–liquid system through boil-

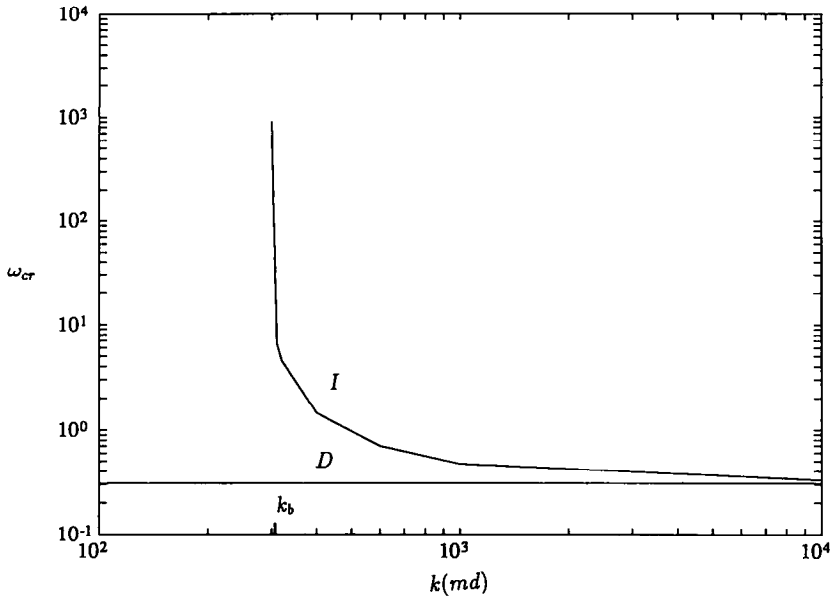

FIG. 4. Critical heat flux vs permeability for the two cases (I corresponds to top cooling, D to bottom heating).

ing by a gradual increase of the heating rate. The liquid pressure is nearly constant, thus the vapor pressure in region II is always higher and positive. Conduction effects are negligible, therefore ω_0 is an excellent approximation to the critical heat flux for the onset of dryout. By contrast, for the other case, an initially vapor-filled medium is converted to a vapor–liquid system through condensation by a gradual increase of the cooling rate. Now, the vapor pressure at the bottom region I is constant and must decrease upwards. For low enough (but not infinitesimally small) values of k, the vapor pressure decrease is so high that it becomes negative. In such a case, increasing ω cannot prevent the collapse of vapor pressure.

We conclude that the critical heat flux curve is different depending on the direction from which the steady-state counterflow is reached. Boiling (bottom heating), which can be likened to drainage, is rather insensitive to permeability and conduction. Condensation (top cooling), which can be likened to imbibition, depends significantly on both variables. This difference may be used to decide on the direction (cooling vs heating) from which the particular counterflow state of a reservoir was reached.

Some additional remarks are also pertinent. In the geothermal literature, gravity-driven heat pipes have often been used as reservoir models. In many instances a subcooled liquid layer is assumed to exist above the two-phase zone. This requires

$$\omega \geqslant \frac{1}{KR_m A_{III}/\tau_{III}^2}. \tag{6}$$

Several geothermal systems appear to satisfy such counterflow configurations (e.g. Kawah Kamojang [5]). In these cases, however, it is necessary that the region below the top subcooled layer has (significantly) higher permeability, for a VD regime to extend to significant depths, as normally assumed. Otherwise, the preceding analysis would dictate either an LD solution of large extent, if $\omega < \omega_{cr}$, or a short two-phase zone followed by a superheated dry region, if $\omega > \omega_{cr}$. In short, the existence of a long vapor-dominated region overlaid by a subcooled liquid is not possible under steady-state conditions in a homogeneous system.

Configurations of the type studied by Martin *et al.* [6] and Schubert and Straus [3] are more likely. Here $\theta = \pi/2$, while the temperature gradient and the heat flux are negative (from the liquid to the vapor [1]), the integration proceeding from bottom (liquid) to top (vapor). To ensure the existence of an underlying subcooled liquid layer, the heat flux should not exceed an upper limit

$$|\omega| \leqslant \frac{1}{KR_m A_{III}/\tau_{III}^2}. \tag{7}$$

Clearly conduction effects may not be neglected here. A two-branch solution, analogous to Fig. 2, also exists in this case for low enough values of $\varepsilon = \sigma RT_0/L_v P_0 M_w \sqrt{k}$ (see Figs. 9 and 12 of ref. [1]). However, here it is the VD regime that attracts trajectories starting from the liquid side, since equation (7) must be satisfied. This long VD zone is underlaid by a region rich in liquid (the relative extent of which depends on capillarity) and, further below, by a subcooled liquid layer. The so called VAPLIQ geothermal systems (e.g. Los Azufres, Mexico) may well fit to this category of counterflow systems. Their heat fluxes should be quite low due to the above limit. In fact, a typical heat flux is approximately estimated to be 25 times smaller than the Kawah Kamojang system [7].

In summary, we have pointed out that steady-state vapor–liquid counterflow cannot be uniquely determined, unless the past history of the system is known. We have differentiated between bottom heating and top cooling to indicate differences between boiling and geothermal applications. The latter differ with respect not only to saturation values, but also to critical heat fluxes. Nevertheless some unresolved issues still exist regarding vapor- or liquid-dominated solutions in the range $\omega < \omega_{cr}$. Finally, we have ruled out the possibility of a VD regime underlying a subcooled liquid in a homogeneous system, but found consistent the reverse configuration at low heat fluxes.

Acknowledgements—This work was partly supported by DOE Contract DE-FG22-90BC14600, the contribution of which is gratefuly acknowledged.

REFERENCES

1. C. Satik, M. Parlar and Y. C. Yortsos, A study of steady-state steam-water counterflow in porous media, *Int. J. Heat Mass Transfer* **34**, 1755–1771 (1991).
2. K. S. Udell, Heat transfer in porous media considering

phase change and capillarity—the heat pipe effect, *Int. J. Heat Mass Transfer* **28**, 485–495 (1985).
3. G. Schubert and J. M. Strauss, Steam–water counterflow in porous media, *J. Geophys. Res.* **84, B4**, 1621–1679 (1979).
4. H. H. Bau and K. E. Torrance, Boiling in low permeability porous materials, *Int. J. Heat Mass Transfer* **25**, 45–54 (1982).
5. J. M. Strauss and G. Schubert, One dimensional model of vapor dominated geothermal systems, *J. Geophys. Res.* **86, B10**, 9433–9438 (1981).
6. J. C. Martin, R. E. Wegner and F. J. Kelsey, One dimensional convective and conductive geothermal heat flow, *Proc. 2nd Workshop Geothermal Reservoir Engng*, Stanford, California, 1–3 December (1976).
7. E. R. Iglesias and V. M. Arellano, Vapliq hydrothermal systems and the vertical permeability of Los Azufres, Mexico, geothermal reservoir, *Proc. 13th Workshop Geothermal Reservoir Engng*, Stanford, California, 19–21 January (1988).

Int. J. Heat Mass Transfer. Vol. 36, No. 1, pp. 231–232, 1993
Printed in Great Britain

0017–9310/93 $5.00 + 0.00

Frequency response of constant-current film anemometers

ANTHONY DEMETRIADES
Department of Mechanical Engineering, Montana State University, Bozeman, MT 59715, U.S.A.

(*Received* 6 *May* 1991 *and in final form* 10 *December* 1991)

TURBULENCE research in high-speed flows has motivated several new measuring methods [1–3], and has also recruited some older techniques already in use for low-speed flows such as thermoelement anemometers ('hot wires' and 'hot films'). Among the latter, film anemometers are especially attractive because their structural rigidity makes them durable in the hostile surroundings of hypervelocity streams. In such environments, however, film anemometers must also demonstrate the proper response to high-frequency signals. The frequency response of flow-immersible film probes therefore acquires new importance and is discussed in this note.

The fundamentals of this problem were addressed long ago by Ling [4] and Ling and Hubbard [5]. The thermal inertia of the thermoelement alone, without a supporting substrate, causes a signal attenuation of 6 db per frequency octave; Ling [4] showed that with a conducting substrate, the attenuation decreases to 3 db octave^{-1}, without, however, presenting the non-dimensional variables and their range for which this conclusion is valid. Since then, moreover, other workers [6–8] have found that the film-probe response can in fact be a very complex function of the frequency, depending on the thermal boundary conditions and the operating constraints (e.g. 'constant-temperature' or 'constant-current' operation). There exists, therefore, some confusion about the basic rules and parameters controlling the response of film anemometers, including those of simple geometry. In this note we are interested in the generic geometry of the long cylindrical probe, parallel to the flow and with a very small metallic film deposited on its sharpened upstream end. For such probes, which have been successfully operated at constant current at hypersonic speeds [9], the response to high-frequency flow fluctuations is especially critical.

The present analysis, details of which appear in ref. [10], aimed at finding the identity and range of the non-dimensional parameters for which the 3 db octave^{-1} response prevails. In common with most previous approaches, the analysis views the film to be so thin that it practically coincides with the surface of the substrate. The power balance equation for the film includes the ohmic heating, the convective heat exchange with the flow and the conductive exchange with the substrate. Radiation is neglected, and the heat flow in the substrate is one-dimensional. The film–substrate system receives a heat input from the flow which fluctuates with a magnitude much smaller than its corresponding mean level. The fluctuations, which may be due to temperature or Reynolds number changes, are assumed stationary and thus decomposable into Fourier components.

Without thermal lag, the film output as a function of time t would be $e_i \sin \omega t$ due to the Fourier component of frequency ω, where e_i stands for the film temperature, or for some electrical property such as its voltage at constant current. The thermal lag distorts this output into $e_o \sin(\omega t + \phi)$. The present analysis gives the following solutions for e_o and ϕ:

$$\frac{e_o}{e_i} = \frac{1}{[(\omega\tau + Q\sqrt{(\omega\tau)})^2 + (1 + Q\sqrt{(\omega\tau)})^2]^{1/2}} \tag{1}$$

$$\phi = \tan^{-1} \frac{\tau\omega + Q\sqrt{(\omega\tau)}}{1 + Q\sqrt{(\omega\tau)}} \tag{2}$$

which are plotted in Figs. 1 and 2 respectively.

Equations (1) and (2) conveniently separate the effects of the film itself from those of the substrate, upon the attenuation factor e_o/e_i and phase lag ϕ. The film is represented by its 'inherent' time constant τ caused by its finite heat capacity ε (energy per degree). This time constant also depends on the film lateral dimension ('width') w, the fluid thermal conductivity at stagnation conditions k_o, the ratio of 'cold' (unheated or equilibrium) to heated resistance R_e/R, the film Nusselt number N and the logarithmic derivative $N_r = (r/N)(\partial N/\partial r)$ of N relative to $r = (R/R_e - 1)$:

$$\tau = \frac{\varepsilon}{wk_o N\left(\dfrac{R_e}{R} + N_r\right)}. \tag{3}$$

This expression is, in fact, the classical one for the time constant of any convection-controlled thermoelement such as 'hot wire' anemometers [11].

The effect of the substrate enters via the non-dimensional 'loss factor' Q, which depends on the substrate conductivity, density and specific heat, k_s, ρ_s, and c_s respectively:

$$Q = \left[\frac{1}{2N}\frac{k_s}{k_o}\frac{\rho_s c_s}{\rho_f c_f}\frac{h}{d}\right]^{1/2}. \tag{4}$$

The film is also represented in equation (4) by its dimensions (height h and depth or thickness d) and material density ρ_f and specific heat c_f. Note that the theory admits a finite mass